Big1 is a newly identified autophagy regulator that is critical for a fully functional V-ATPase

Yuchen Lei[a,†], Ying Yang[a,†], Zhihai Zhang[a], Ruoxi Zhang[b], Xinxin Song[b], Sami N. Malek[c], Daolin Tang[b], and Daniel J. Klionsky[a,*]

[a]Life Sciences Institute and Department of Molecular, Cellular and Developmental Biology, University of Michigan, Ann Arbor, MI 48109-2216; [b]Department of Surgery, University of Texas Southwestern Medical Center, Dallas, TX 75390; [c]Internal Medicine, Division of Hematology and Oncology, University of Michigan, Ann Arbor, MI 48109-0936

ABSTRACT **The vacuolar-type H^+-translocating ATPase (V-ATPase) is the major proton pump for intraorganellar acidification. Therefore, the integrity of the V-ATPase is closely associated with cellular homeostasis, and mutations in genes encoding V-ATPase components and assembly factors have been reported in certain types of diseases. For instance, the recurrent mutations of *ATP6AP1*, a gene encoding a V-ATPase accessory protein, have been associated with cancers and immunodeficiency. With the aim of studying V-ATPase–related mutations using the yeast model system, we report that Big1 is another homologue of ATP6AP1 in yeast cells, and we characterize the role of Big1 in maintaining a fully functional V-ATPase. In addition to its role in acidifying the vacuole or lysosome, our data support the concept that the V-ATPase may function as part of a signaling pathway to regulate macroautophagy/autophagy through a mechanism that is independent from Tor/MTOR.**

Monitoring Editor
Michael Marks
Children's Hospital of Philadelphia

Received: Apr 26, 2024
Revised: Aug 29, 2024
Accepted: Aug 29, 2024

New Hypothesis

SIGNIFICANCE STATEMENT

- The V-ATPase accessory protein ATP6AP1 is mutated in multiple diseases. Voa1 and Big1 are identified as two yeast homologues; the function of Big1 is unknown, and whether ATP6AP1 or Big1 can regulate autophagy is unclear.
- Big1 is critical in maintaining a fully functional V-ATPase. Furthermore, knocking down *BIG1* induces autophagy even when Tor is active. Increased autophagy is also seen in human cells when ATP6AP1 is knocked down.
- This study identifies a new protein that functions in V-ATPase assembly and provides support for Tor-independent autophagy. In addition, cancer-associated mutations in V-ATPase may affect autophagy.

This article was published online ahead of print in MBoC in Press (http://www.molbiolcell.org/cgi/doi/10.1091/mbc.E24-04-0189) on October 1, 2024.

†These authors contribute equally.

Conflicts of interest: The authors declare no financial conflict of interest.

Author contributions: D.J.K., Y.L., Y.Y., X.S., S.N.M., and D.T. conceived and designed the experiments; D.J.K., Y.L., Y.Y., Z.Z., R.Z., X.S., S.N.M., and D.T. analyzed the data; D.J.K., Y.L., and Y.Y. drafted the article; Y.L., Y.Y., Z.Z., R.Z., and X.S. performed the experiments; Y.L. prepared the digital images.

*Address correspondence to: Daniel J. Klionsky (klionsky@umich.edu).

Abbreviations used: AID*, auxin-inducible degron; ATG, autophagy related; BafA1, bafilomycin A1; BiFC, bimolecular fluorescence complementation; DMSO, dimethyl sulfoxide; ER, endoplasmic reticulum; FL, follicular lymphoma; GFP, green fluorescent protein; IAA, indole-3-acetic acid; IP, immunoprecipitation; ORF, open reading frame; PAGE, polyacrylamide gel electrophoresis; PCR, polymerase chain reaction; SD-N, nitrogen-starvation medium; V-ATPase, vacuolar type H^+-translocating ATPase.

INTRODUCTION

The vacuolar-type H^+-translocating ATPase (V-ATPase) is a conserved and ubiquitously expressed protein complex, which is the main regulator of intraorganellar acidification. The V-ATPase is a multi-subunit complex composed of two large domains, the cytosolic V_1 domain, which hydrolyzes ATP, and the membrane-embedded V_0 domain, which transports protons. The V_0 and V_1 domains can assemble separately and the assembly of the two domains is highly regulated (Chen *et al.*, 2022). In yeast cells, the assembly of the V_0 domain components occurs in the endoplasmic reticulum (ER) membrane and depends on several assembly factors residing in the ER, including integral membrane proteins Vma12 and Vma21 and the peripheral membrane protein Vma22 (Hill and Stevens, 1994; Hill and Stevens, 1995; Jackson and Stevens, 1997; Malkus *et al.*, 2004; Wang *et al.*, 2023). In addition, Voa1 has also been shown to participate in the assembly of the V_0 domain (Ryan *et al.*, 2008). The assembled V_0 domain is transported to the Golgi membrane where the V_1 domain assembles with it (Wang *et al.*, 2023). Even though V-ATPase assembly in mammalian cells is less well studied than in yeast cells, homologues of most of the yeast V-ATPase assembly factors have been identified and several studies resolving mammalian V-ATPase structure have shed light on V-ATPase assembly in more complex eukaryotes (Wang *et al.*, 2020; Wang and Rubinstein, 2023).

As the main proton pump responsible for the acidification of endomembrane compartments, including the lysosome and vacuole, the V-ATPase plays a critical role in autophagy, a conserved degradation pathway depending on the vacuole/lysosome; V-ATPase–mediated vacuolar/lysosomal acidification affects the fusion of the autophagosome (the double-membrane vesicle that transports autophagic cargo) and the vacuole/lysosome (Lee *et al.*, 2010), and the dysregulation of vacuolar/lysosomal pH can result in the disrupted lysosomal degradation of autophagic cargos (Han *et al.*, 2022). In addition, the V-ATPase also plays a significant role in other types of autophagy, such as xenophagy and noncanonical autophagy, independent from its major function in mediating acidification (Xu *et al.*, 2019; Hooper *et al.*, 2022; Lei and Klionsky, 2022). More importantly, mutations in, and the dysregulation of, the V-ATPase have been linked with multiple human diseases, such as cancer, neurodegenerative disorders, and infectious diseases (Colacurcio and Nixon, 2016; Chen *et al.*, 2022).

Various genes encoding V-ATPase structural components and assembly factors have been demonstrated to be highly mutated in follicular lymphoma (FL), including *VMA21* and *ATP6V1B2*, and some mutations cause abnormal autophagy (Wang *et al.*, 2019; Wang *et al.*, 2022). *ATP6AP1/Ac45*, one of the V-ATPase accessory proteins in the mammalian system, is also frequently mutated in FL cases (Okosun *et al.*, 2016; Wang *et al.*, 2022). In addition, *ATP6AP1* is highly mutated in other cancers and diseases, such as granular cell tumors and immunodeficiency (Jansen *et al.*, 2016; Pareja *et al.*, 2018), suggesting the importance of this gene. Given the close connection between the V-ATPase and autophagy, it is possible that ATP6AP1 functions as an autophagy regulator and that these mutations may result in an alteration in autophagy activity, thereby contributing to disease development or progression. Thus, a better understanding of mutations in genes encoding the V-ATPase and/or its assembly factors may provide useful insights for designing therapeutic approaches.

As the V-ATPase is essential for eukaryotic cell viability except in fungi (Ryan *et al.*, 2008) and the vacuole, the equivalent organelle to the lysosome, is relatively large, yeast cells serve as a good model organism to study the V-ATPase. Therefore, we decided to examine the role of ATP6AP1 in autophagy by studying its homologue in yeast cells. In this study, we determined that Big1, a largely uncharacterized protein, is a second homologue of ATP6AP1 and is important for a fully functional V-ATPase in yeast cells. In addition, we found that the removal of Big1 results in autophagy induction. Similarly, the knockdown of *ATP6AP1* in human cells also causes increased autophagy, suggesting that the V-ATPase may function as a signal in regulating bulk autophagy besides its role in acidifying the lysosome or vacuole.

RESULTS AND DISCUSSION

Yeast Big1 has a function similar to mammalian ATP6AP1

Using HHpred, a server for protein homology detection and structure prediction (https://toolkit.tuebingen.mpg.de/tools/hhpred) (Soding *et al.*, 2005), we determined that the sequence of the yeast protein Big1 has significant similarity to the N terminus of ATP6AP1 (E = 3.8e-22) (Figure 1A; Supplemental Figure S1). In addition, Voa1 has also been shown to have significant similarity to both the N and C termini of ATP6AP1 (E = 0.045 and 3.4e-9, respectively). Compared with Voa1, which has been defined as a V-ATPase assembly factor with known structure and localization, very few studies have focused on Big1. The current available information concerning Big1 is that it is located in the ER and is required for the synthesis of β-l,6-glucan, an essential polymer involved in the cell wall attachment of many surface mannoproteins (Azuma *et al.*, 2002). We examined the localization of Big1 tagged with green fluorescent protein (GFP) relative to the ER marker Sec63-RFP and found substantial overlap (Figure 1B), confirming that Big1 resides in the ER.

Given the similarity between sequences of Big1 and ATP6AP1, we suspected that Big1 may also function in V-ATPase assembly. Yeast cells with deficient V-ATPase activity are viable but exhibit a Vma^- phenotype, characterized by the inability to grow in medium buffered to pH 7.5 and/or in the presence of a higher extracellular concentration of calcium or heavy metals (Sambade *et al.*, 2005); culture medium at pH 5.0 suppresses the growth defect. Vma21 plays a major role in V-ATPase assembly (Hill and Stevens, 1994). For example, the phenotype associated with the *voa1* deletion is strongly exacerbated in cells with partially defective Vma21 (Ryan *et al.*, 2008). Vma21 requires a C-terminal dilysine motif to be retained in the ER; when the dilysine is mutated to diglutamine (Vma21[QQ]), Vma21 is mislocalized resulting in reduced V-ATPase assembly and activity (Ryan *et al.*, 2008). Accordingly, we generated *big1*Δ cells in a Vma21[QQ] background. Compared with the wild-type cells, *big1*Δ *vma21[QQ]* cells showed a growth deficiency on a YPD plate buffered to pH 7.5 in the presence of 35 mM calcium. In contrast, there was no significant difference in growth on YPD buffered to pH 5.0. The growth phenotype was partially rescued by adding back Big1 or, to a lesser extent, human ATP6AP1 driven by the yeast *ZEO1* promoter (Figure 1C). Expressing the N terminus of ATP6AP1, corresponding to the region that is homologous to Big1, recues the growth phenotype better than full-length ATP6AP1, which may be due to inefficient Kex2/furin cleavage in yeast cells, an important step for the full function of

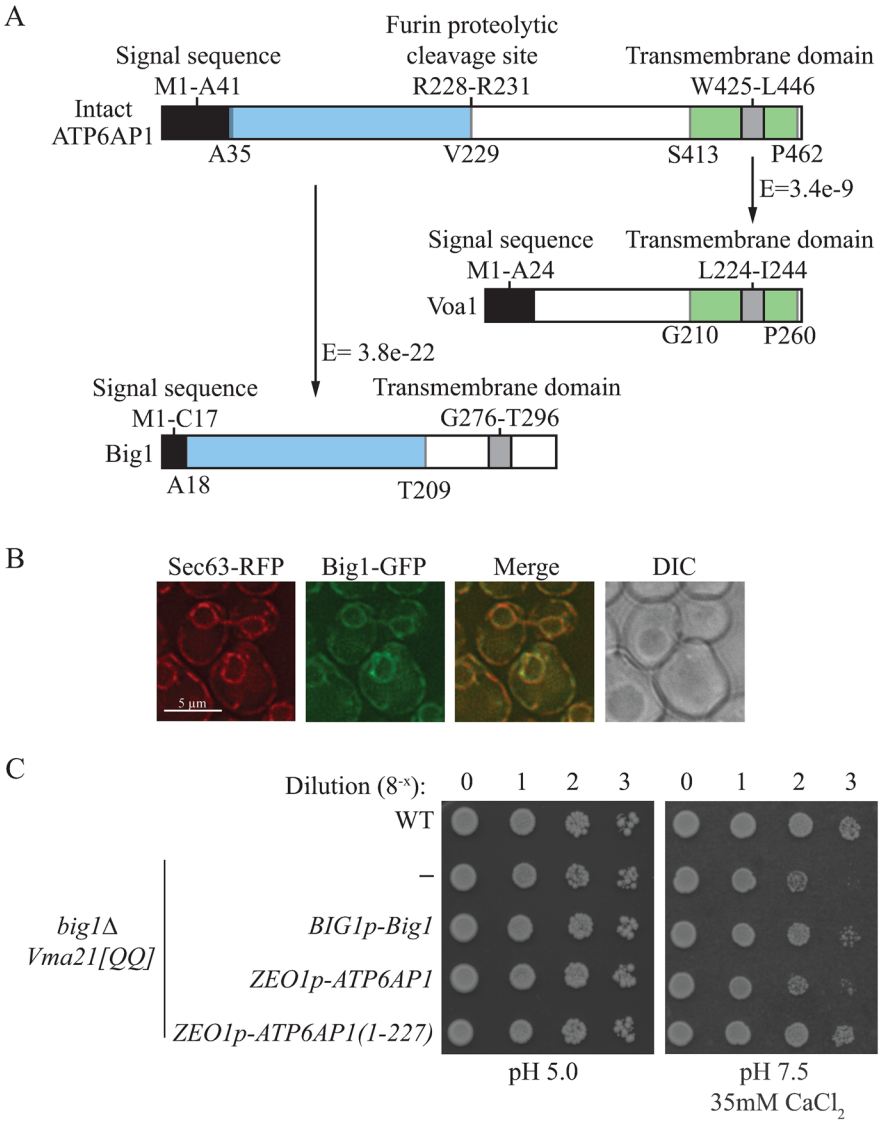

FIGURE 1: Big1 functions similarly to ATP6AP1. (A) Overview of the regions of ATP6AP1 that are homologous to the yeast proteins Voa1 (green) and Big1 (blue). The features of the proteins, including the signal sequence (black), transmembrane domain (gray), and proteolytic cleavage site are based on the information from UniProt (https://www.uniprot.org/) and previous studies. (B) *SEC63-RFP BIG1-GFP* cells were cultured in YPD to midlog phase and images were captured by fluorescence microscopy. DIC, differential interference contrast. (C) Wild-type, *big1*Δ *Vma21[QQ]*, and *big1*Δ *Vma21[QQ]* cells transformed with a plasmid encoding Big1 driven by the endogenous promoter or full-length ATP6AP1 or the first 227 amino acids of ATP6AP1 driven by the *ZEO1* promoter were cultured in YPD to midlog phase. The colony dot blot was performed as described in the *Materials and Methods*.

ATP6AP1 (Louagie *et al.*, 2008) (Figure 1C). This finding suggests that Big1 is one of the functional homologues of ATP6AP1 and may function in V-ATPase assembly in yeast.

Big1 depletion leads to less V-ATPase on the vacuole and deficient enzyme activity

Some studies classify *BIG1* as an essential gene (Azuma *et al.*, 2002; Morgan *et al.*, 2019), and *big1*Δ cells grow slowly (doubling time being ~2 h). Thus, to avoid potential indirect effects brought about by the deletion of *BIG1*, we took advantage of the auxin-inducible degron (AID*) system to conditionally knock down *BIG1* expression. This system is well established in yeast cells to temporally control gene expression by mediating proteasomal degradation of targeted proteins in an auxin-dependent manner (Nishimura *et al.*, 2009). Therefore, these cells can be maintained as essentially wild type for normal growth and Big1 can be removed in a temporal manner. The phenotype of V-ATPase assembly defects is cumulative, and only newly synthesized complexes are affected; thus, some time is necessary for the phenotype to be strong enough to be detected. Accordingly, we treated the Big1-AID* cells with 300 µM indole-3-acetic acid (IAA) for 12 h before collecting samples, which is enough for essentially complete loss of detectable Big1 (Figure 2A). To directly determine the impact on V-ATPase assembly after the knockdown of *BIG1*, yeast vacuoles were isolated, and the protein levels of some V-ATPase components were detected by western blot (Figure 2B). Compared with the control cells treated with DMSO, we observed that vacuolar protein levels of Vph1, a

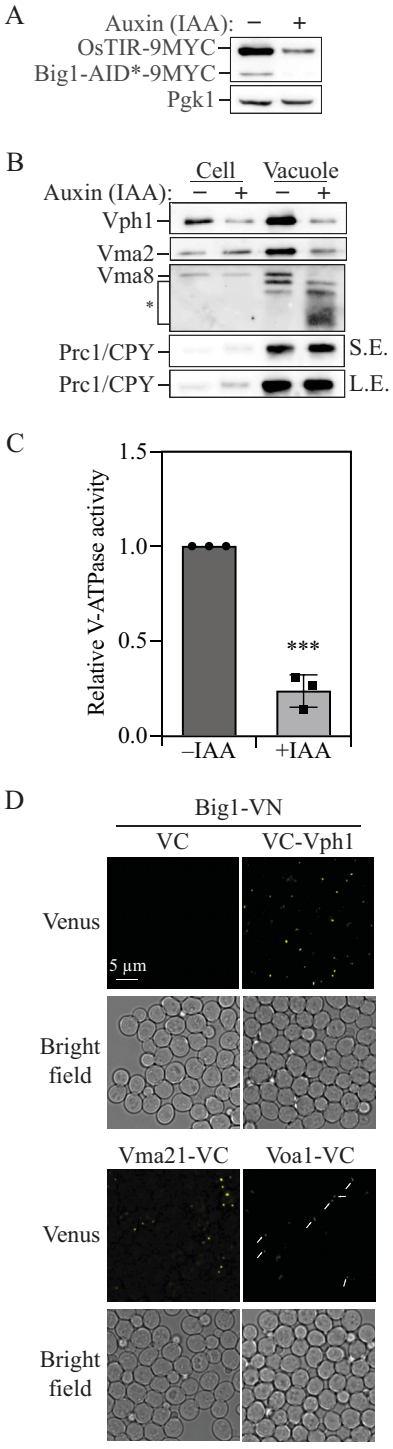

FIGURE 2: Big1 plays a role in V-ATPase assembly. (A and B) Big1-AID* cells were cultured in YPD overnight until midlog phase then diluted and treated with DMSO or IAA for 12 h. (A) Cell lysates were prepared and (B) vacuoles were isolated. These samples were subject to SDS–PAGE and analyzed by western blot. Pgk1 was used as a loading control in A. Prc1/CPY was used as a confirmation of vacuole accumulation and as a loading control for the vacuole amount in B. * in B indicates nonspecific binding. L.E., long exposure; S.E., short exposure. (C) The V-ATPase activity of vacuoles prepared in B was measured as described in *Materials and Methods*. The IAA treatment group was normalized to the control group. Average values ± s.d. of $n = 3$ independent experiments are shown. ***$p < 0.001$. (D) Cells expressing Big1-VN were transformed with plasmids expressing VC or VC-tagged proteins as indicated in the figure. These cells were cultured in YPD to midlog phase. Images were captured by fluorescence microscopy and all z-sections were projected. The puncta in cells expressing Big1-VN and Voa1-VC are highlighted by white arrows.

V_0 domain component, and Vma2 and Vma8, two V_1 domain components, significantly decreased in the cells treated with IAA. Vph1 levels were also decreased in the total cell extract, which fits with the observation that this subunit is unstable when V-ATPase assembly is defective (Ryan *et al.*, 2008). In addition, using isolated vacuoles, V-ATPase activity was measured in a bafilomycin A_1 ($BafA_1$)-dependent manner. Consistent with the protein level, the V-ATPase activity was significantly reduced in the Big1-AID* cells treated with IAA relative to the control group (Figure 2C). These results indicate that the removal of Big1 leads to a reduced level of V-ATPase subunits on the vacuole, suggesting that Big1 is critical in maintaining the normal level and function of the V-ATPase.

We further determined whether Big1 interacts with V-ATPase. We used the bimolecular fluorescence complementation (BiFC) assay, which is based on the association between fragments of a fluorescent protein when they are tethered in the same macromolecular complex. In this assay, two fragments, VN and VC of Venus, a yellow fluorescent protein, are fused to two proteins of interest. The interaction between the proteins facilitates the association between the VN and VC chimeras to produce a bimolecular fluorescent complex (Kerppola, 2006). We tagged the VN fragment to Big1 (Big1-VN) and VC to the V-ATPase component Vph1 (VC-Vph1), and assembly factors, including Vma21 (Vma21-VC) and Voa1 (Voa1-VC) and imaged cells by fluorescence microscopy. Clear YFP puncta were observed in the Big1-VN cells expressing VC-Vph1 or Vma21-VC (Figure 2D). Even though the puncta were not as bright, they were also detected in the Big1-VN cells expressing Voa1-VC (Figure 2D). The faint puncta in these strains could be explained by the localization of Voa1 in the middle of the V-ATPase Vma3/c-ring (Roh *et al.*, 2018), which make the interaction or colocalization hard to detect by the BiFC assay. The interaction between Big1 with V-ATPase components and assembly factors is similar to Vma21, which can interact with Vph1 and to a lesser extent Voa1 (Supplemental Figure S2A) (Barua *et al.*, 2022). We further examined the site of these interactions and found that most of those between Big1 and Vph1 occurred at the ER-vacuole contact site, whereas more of the interactions between Vma21 and Voa1 were on the ER (Supplemental Figure S2B). In addition, the interaction between Big1 and Vma21 or Vph1 could be detected by co-immunoprecipitation (Supplemental Figure S2, C and D). These results demonstrate that Big1 interacts with some of the V-ATPase components and assembly factors and may function in facilitating V-ATPase assembly though these interactions.

Big1 depletion induces autophagy

Given the close association between V-ATPase and autophagy, it is possible that Big1 could be an autophagy regulator in yeast cells. Using the Big1-AID* strain, we decided to investigate the impact on autophagy brought about by the reduced expression level of *BIG1*. After treating the Big1-AID* cells with IAA for 12 h under nutrient-rich conditions, the cells were transferred to nitrogen-starvation medium (SD-N) and IAA treatment was continued in this condition to maintain the *BIG1* expression at a minimal level. We utilized the GFP-Atg8 processing assay, where Atg8 is tagged with GFP at its N terminus, to evaluate autophagy flux. The principle of

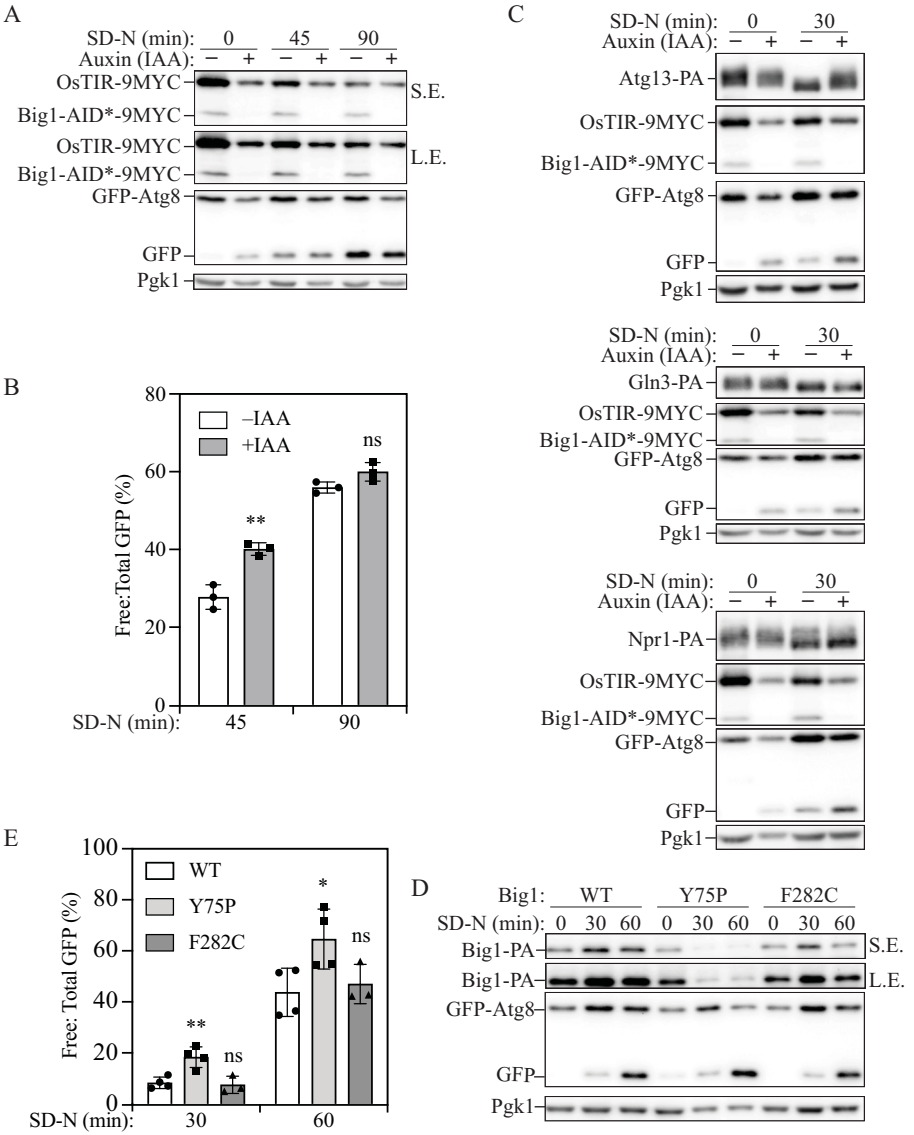

FIGURE 3: Knockdown of Big1 induces autophagy. (A) Big1-AID* cells expressing the *pRS405-CUP1p-GFP-ATG8* plasmid were cultured in YPD overnight until the midlog phase then diluted and treated with DMSO or IAA for 12 h (SD-N 0 min) and shifted to SD-N for 45 and 90 min while maintaining DMSO or IAA treatment. Cell lysates were prepared, subjected to SDS–PAGE, and analyzed by western blot. Pgk1 was used as a loading control. (B) Quantification of free to total GFP (GFP + GFP-Atg8) ratio after 45- and 90-min starvation. Average values ± s.d. of $n = 3$ independent samples in A are shown. (C) Big1-AID* cells with PA-tagged Atg13, Gln3, or Npr1 were cultured in YPD overnight until midlog phase, diluted and treated with DMSO or IAA for 12 h (SD-N 0 min) then shifted to SD-N for 30 min with DMSO or IAA treatment. Cell lysates were prepared, subjected to SDS–PAGE, and analyzed by western blot. Pgk1 was used as a loading control. A representative blot from three repeats of each cell is shown. PA, protein A. (D) Cells with wild-type or mutant *BIG1* were cultured in YPD overnight until midlog phase (SD-N 0 min) and then shifted to SD-N for 30 and 60 min. Cell lysates were prepared, subjected to SDS–PAGE and analyzed by western blot. Pgk1 was used as a loading control. (E) Quantification of free to total GFP (GFP + GFP-Atg8) ratio after 30- and 60-min starvation. Average values ± s.d. of $n = 3$ or 4 independent samples in D are shown. *$p < 0.05$, **$p < 0.01$; ns, not significant. L.E., long exposure; S.E., short exposure.

this assay is that the GFP-Atg8 on the inner membrane of the autophagosome will be delivered to the vacuole after the autophagosome fuses with this compartment. Within the vacuole, Atg8 will be degraded by vacuolar hydrolases, but GFP is more resistant to degradation. Therefore, free GFP is generated and the conversion of GFP-Atg8 to free GFP reflects autophagy flux. After the removal of Big1 by treating the cells with IAA for 12 h, we noticed the GFP-Atg8 cleavage even before starvation (Figure 3A; 0 min, +IAA), indicating that autophagy was activated by the reduced Big1 protein level under nutrient-rich conditions; autophagy is normally kept at a low basal level until cells are stressed. This induced autophagy can be suppressed by adding back another copy of Big1 from a plasmid (Supplemental Figure S3A), indicating that this phenotype resulted solely from the removal of Big1. To provide further support for the induction of autophagy under nutrient-rich conditions, we measured the expression level of some *ATG* (autophagy

related) genes. We chose *ATG1*, *ATG7*, *ATG8*, *ATG9*, and *ATG41*, which are all essential for the efficient activation of autophagy, because each of these genes shows an increase in expression upon autophagy induction and the level of Atg7, Atg8, and Atg9 clearly correlates with autophagy activity (Bernard *et al.*, 2015; Yao *et al.*, 2015). The expression of each of these genes increased after IAA treatment compared with the control DMSO-treated cells in the nutrient-rich medium (Supplemental Figure S3B). This result confirmed the induction of autophagy by the removal of Big1 protein under nutrient-rich conditions. After starvation, the autophagy activity also showed an increase in the IAA treatment group, however, to a lesser extent compared with the cells in growing conditions (Figure 3, A and B, 45 and 90 min). This finding fits with the general observation that it is easier to detect positive effects of mutations on autophagy under growing conditions when autophagy is typically downregulated (Bartholomew *et al.*, 2012); under starvation conditions, autophagy is highly upregulated due to the inhibition of various negative factors, making it difficult to detect the relatively smaller increase in activity such as can be seen in nutrient-rich conditions. In addition, when we followed the autophagy induction across the 12-h IAA treatment, we found that the GFP-Atg8 cleavage under growing conditions occurred after 4-h IAA treatment and a peak occurred at ~8 h (Supplemental Figure S3C). These results suggest that the removal of Big1 induces autophagy and that the primary impact is seen under nutrient-rich conditions.

One reason that autophagy is maintained at a low basal level when nutrients are replete is due to the activation of Tor, a key nutrient sensor and the primary negative regulator of autophagy in yeast cells. Activated Tor phosphorylates various Atg proteins including Atg1 and Atg13 (Kamada *et al.*, 2010) and inhibits the formation of the principle autophagy initiating complex consisting of Atg13, Atg1, and Atg17-Atg31-Atg29 (Kabeya *et al.*, 2005; Liu *et al.*, 2016). Because we saw the abnormal activation of autophagy under nutrient-rich conditions after knocking down the expression of *BIG1*, we next analyzed the Tor activation status by analyzing the phosphorylation of Atg13, Gln3, and Npr1, which are phosphorylated in a Tor-dependent manner (Schmidt *et al.*, 1998; Crespo *et al.*, 2002; Chang and Neufeld, 2009). Accordingly, we prepared protein extracts and analyzed them by SDS–PAGE and western blot; all of these proteins migrate at a higher molecular mass when phosphorylated. Under nutrient-rich conditions, Atg13, Gln3, and Npr1 migrated at a higher position, suggesting the phosphorylation of these three proteins in Big1-AID* cells treated with either DMSO or IAA; in contrast, there was an increase in mobility on the gel when cells were starved, corresponding to a decrease in phosphorylation (Figure 3C). This finding indicates that Tor was activated under nutrient-rich conditions regardless of the presence of the Big1 protein. That is, induction of autophagy following the addition of IAA did not occur due to inactivation of Tor. To further support the conclusion that Tor is activated under nutrient-rich conditions, we treated the cells with rapamycin for 30 min after 12-h DMSO or IAA treatment. In the control group, rapamycin resulted in a higher mobility of Atg13, Gln3, and Npr1, indicating their dephosphorylation. In the cells with IAA treatment, the bands corresponding to Gln3 and Npr1 shifted to the same position as the control group, suggesting that these two proteins were dephosphorylated to the same level (Supplemental Figure S4A). However, with rapamycin treatment, even though Atg13 had a higher mobility, it still migrated at a position of higher mass in the *BIG1* knockdown cells compared with the control cells, indicating that Atg13 was phosphorylated by kinases other than Tor when Big1 was removed (Supplemental Figure S4A).

In addition, we also noticed a partial phosphorylation of Atg13 in Big1-AID* cells treated with IAA after 30 min of starvation, relative to the control (Figure 3C). To determine whether Tor was fully inactive after starvation, we further treated the cells with rapamycin for 20 min following the 30-min starvation. In the cells with and without IAA treatment, rapamycin did not cause further dephosphorylation of Atg13, Gln3, and Npr1 (Supplemental Figure S4, B–D), indicating Tor1 was fully deactivated by 30 min of nitrogen starvation, and Tor was therefore not responsible for the partial phosphorylation of Atg13 under starvation conditions when Big1 was depleted. A similar result was seen with Sch9, another target of Tor (Urban *et al.*, 2007). Due to the large size and multiple phosphorylation sites of this protein, we used SDS–PAGE with Phos-tag to better determine the phosphorylation status of Sch9 (Supplemental Figure S4, E and F). Sch9 displayed hyperphosphorylation in the cells without Big1, and rapamycin treatment or nitrogen starvation only resulted in partial dephosphorylation, indicating that Sch9 may be phosphorylated by kinases other than Tor under this condition. All these results indicate that Tor activation only depends on the nutrient status, but not the existence of Big1. A reduced *BIG1* expression level can induce autophagy even when Tor was active, and kinases other than Tor appear to be involved in controlling this pathway.

Because a previous study suggests that Big1 is important for the integrity of the cell wall (Azuma *et al.*, 2002), we wanted to eliminate the possibility that autophagy was induced due to osmotic stress. To relieve the possible osmotic pressure brought about by Big1 removal, 0.6 M sorbitol was added to the medium to maintain iso-osmotic conditions. However, even with sorbitol present, autophagy was still activated in the Big1-AID* strain after adding IAA (Supplemental Figure S3C). Therefore, the autophagy induction observed after the knockdown of *BIG1* is not likely to result from osmotic stress. Instead, the deficient V-ATPase after Big1 removal may function as a signal to activate autophagy independent from the Tor pathway.

A cancer-associated mutation in Big1 induces autophagy

From the sequencing data of pure FL B-cell DNA isolated from flow-sorted FL B cells in FL cases as described in a previous study (Wang *et al.*, 2022), several mutations in *ATP6AP1* were discovered. We focused on two missense mutations that lead to an amino acid change at the N terminus of ATP6AP1 (c.269T>C/T, p.90L>L/P and c.938A>G, p.313Y>C). Sequence alignment showed that the ATP6AP1 L90P and Y313C correspond to yeast Big1 Y75P and F282C, respectively. To study the effect of these mutations on autophagy, we generated these mutations at the genomic *BIG1* locus and examined autophagy activity using the GFP-Atg8 processing assay. Cells carrying the Y75P mutation in Big1 showed a higher autophagy flux after starvation for 30 and 60 min while cells with the F282C mutation did not show a significant change compared with the wild type, as quantified by the free to total GFP (GFP + GFP-Atg8) ratio (Figure 3, D and E). In addition, we noticed that mutant cells have a lower vacuolar level of some V-ATPase components (Supplemental Figure S5A), which is consistent with what we observed when *BIG1* expression was knocked down using the AID* system. We also tested the V-ATPase in the cells carrying the Y75P mutation in Big1, but did not see significantly reduced activity in these mutant cells even though V-ATPase protein levels on the vacuole decreased (Supplemental Figure S5B). A possible explanation is that the V-ATPase protein level on the vacuole in the $Big1^{Y75P}$ mutant was not decreased as severely as seen with Big1 depletion when using the AID system (Figure 2B). In addition, the

Big1^{Y75P} mutation is chronic compared with the acute depletion of Big1-AID*; thus, the Big1^{Y75P} mutant cells may have acquired some type of compensation/suppression, and, therefore, the V-ATPase phenotype would be more difficult to observe.

Because we noticed that the Y75P mutation resulted in a lower protein level compared with the wild-type protein (Figure 3D), we decided to determine whether the reduced protein level was the only cause of the autophagy phenotype that we observed. To rescue the mutant protein level, we transformed a plasmid carrying *CUP1* promoter-driven Big1^{Y75P} into the cells carrying this mutation at the endogenous *BIG1* locus (Supplemental Figure S5C). The presence of the Big1^{Y75P} plasmid resulted in a higher protein level of mutant Big1 than seen with the wild-type protein under growing conditions and a similar but slightly higher level during starvation (Supplemental Figure S5D, left). Even though more mutant protein was present, the autophagy activity was still higher than that seen in the wild-type cells, although it was lower than that of the cells only carrying one copy of the mutant gene (Supplemental Figure S5D, right). Therefore, we conclude that the Y75P mutation may lead to the instability of this protein and its degradation, which results in a lower protein level, but at the same time this mutation causes a partial loss of function of Big1, together resulting in the increased autophagy phenotype. Overall, we determined that the cancer-associated Y75P mutation in Big1, corresponding to L90P in human ATP6AP1, induces autophagy and disrupts the normal function of the V-ATPase. These results further support the role of Big1 in V-ATPase function and suggest that some cancer-associated mutations in V-ATPase subunits or assembly factors may affect autophagy.

ATP6AP1 knockdown induces autophagy in mammalian cells

The role of ATP6AP1 in autophagy regulation was also investigated in the human fibrosarcoma cell line HT1080. Here, we used two siRNAs to knock down the expression of *ATP6AP1* and found that both led to a significant decrease compared with the cells treated with control siRNA (Figure 4, A and B). In both cases, with *ATP6AP1* knockdown cells we detected a trend of increasing LC3B-II/Atg8–PE prior to starvation. In addition, compared with the control group, LC3B-II showed a significant increase after starvation (Figure 4, A and B). Furthermore, the level of SQSTM1/p62, a receptor that is degraded through the autophagy pathway, was decreased in the *ATP6AP1* knockdown cells using *siATP6AP1-2* siRNA compared with the control group (Figure 4B). In the case of *ATP6AP1* knockdown cells using si*ATP6AP1-1*, even though the SQSTM1 protein level was not statistically different from the control group, we still observed a trend of decreasing protein after starvation (Figure 4A). These results demonstrate that knockdown of *ATP6AP1* induced autophagy in mammalian cells, which is consistent with the observation in yeast cells.

Because of the high mutation frequency of *ATP6AP1* in multiple human diseases that are closely correlated with autophagy, we explored the role of this V-ATPase assembly factor in autophagy regulation. Through identifying the homologue of ATP6AP1, we focused on Big1, whose function was relatively uncharacterized. In this report, we demonstrated that Big1 plays a critical role in keeping the normal amount and function of V-ATPase on the yeast vacuole and the removal of this protein induces autophagy even under nutrient-rich conditions. Similarly, the knockdown of *ATP6AP1* induced autophagy in the HT1080 cell line.

We proposed that Big1 may function in controlling V-ATPase activity through interacting with the structural components and assembly factors and we did detect such interactions, including with Vph1 and Vma21 (Figure 2D; Supplemental Figure S2, C and D). One feature that distinguishes Big1 from the other known assembly factors is that a large proportion of Big1 is located in the lumen (Supplemental Figure S6A). To better understand whether this lumenal part contributes to Big1 function, we predicted the interaction between Big1 and Vph1 using ColabFold (Supplemental Figure S6B). In the predicted model with the highest ranking, one interface was identified and this interface was located in the lumenal part of both proteins (Supplemental Figure S6C). Therefore, we think that Big1 may cooperate with the other assembly factors, interacting with different components in the V_0 subunit, thus making the V-ATPase more stable (Compton *et al.*, 2006; Roh *et al.*, 2018). A more detailed mechanism of how Big1 functions in V-ATPase assembly or activity may be determined through resolving the structure of this protein.

Besides discovering a new role of Big1 in V-ATPase assembly, we think that one of the most interesting discoveries in this report is the simultaneous activation of Tor and autophagy when *BIG1* expression is knocked down because Tor is considered as the master negative regulator of autophagy. One explanation of this phenotype is that the removal of the Big1 protein causes deficient V-ATPase, which functions as a signal to induce autophagy. This phenotype is consistent with previous reports; mutations in some V-ATPase components and assembly factors, which result in deficient V-ATPase, lead to increased autophagy activity (Wang *et al.*, 2019; Wang *et al.*, 2022). However, the downstream effector protein/pathway is unknown and requires further investigation. Besides the hyperphosphorylation of Atg13 and Sch9 during nutrient starvation or after rapamycin treatment (Figure 3C; Supplemental Figure S4, A, B, E, and F), we also noticed a mass shift of Atg1 in the yeast cells with *BIG1* depleted after starvation, which might indicate an alteration in Atg1 phosphorylation (Supplemental Figure S4G). Therefore, we speculate that a kinase may be activated when Big1 is removed. Snf1, the AMP-activated serine/threonine protein kinase/AMPK in yeast is involved in autophagy (Hu *et al.*, 2019). Accordingly, we tested the activation of Snf1 when Big1 was removed by IAA treatment (Supplemental Figure S7). Even though we noticed a decreased total protein level in the IAA treatment group, possibly caused by the 3HA tagging (Saiz-Baggetto *et al.*, 2017), the proportion of activated Snf1 (p-Snf1) was significantly higher than in the control group (Supplemental Figure S7B), indicating it could be the cause of hyperphosphorylated Atg13 and Sch9. Thus, hyperactivation of Snf1 may be a reason for the induced autophagy but it may not be the only reason. Therefore, determining the mediators of this change in phosphorylation can shed more light on the autophagy regulation pathway under these conditions.

In this study, the regulation of autophagy through ATP6AP1 has been demonstrated and one of the cancer-associated mutations in *ATP6AP1* was shown to induce autophagy, suggesting that further analysis can focus on disease-associated mutations in *ATP6AP1* (Jansen *et al.*, 2016; Pareja *et al.*, 2018; Barua *et al.*, 2022) to determine whether they cause functional changes in this protein and whether the cells carrying these mutations have an abnormal autophagy phenotype. Due to the high mutation frequency of this gene in a wide range of human diseases, these studies will provide us with a deeper understanding of the association between autophagy and human health and may provide new insights in designing new therapeutic strategies.

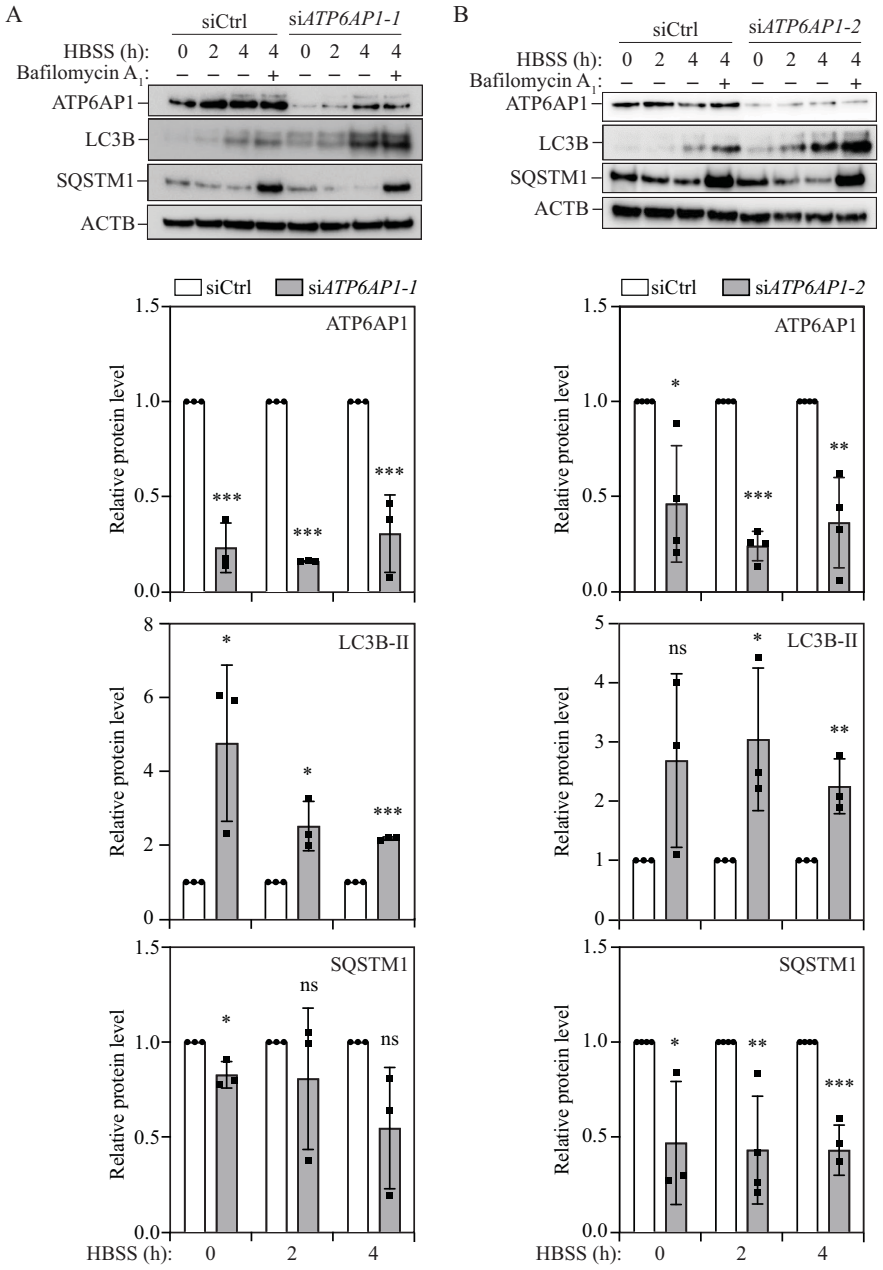

FIGURE 4: Knocking down *ATP6AP1* induces autophagy. Western blot analysis of the indicated protein expression in HT1080 cells after treatment with HBSS in the absence or presence of bafilomycin A_1 (100 nM) for 2–4 h, using (A) *siATP6AP1-1* and (B) *siATP6AP1-2* to knock down the expression of *ATP6AP1*. The quantification of each western blot is shown below. The protein level of ATP6AP1, LC3B-II, and SQSTM1 was first normalized to ACTB, then normalized to the control group at each starvation timepoint. Average values ± s.d. of $n = 3$ or 4 independent samples were used in the quantification. *$p < 0.05$, **$p < 0.01$, ***$p < 0.001$; ns, not significant.

MATERIALS AND METHODS

Yeast strains, media, and growth conditions

Yeast strains used in this study are listed in Supplemental Table S1. Gene deletions were generated according to the standard method (Gueldener *et al.*, 2002). Strains YYY087 (*BIG1[F282C]*), YYY088 (*BIG1[Y75P]*), and ZZH337 (*big1Δ VMA21[QQ]*) were made by mutating *BIG1* or *VMA21* at the corresponding residues on the genome (Gardner and Jaspersen, 2014). Yeast cells were cultured at 30°C in rich medium (YPD; 1% yeast extract, 2% peptone, and 2% glucose) or synthetic minimal medium (SMD; 0.67% yeast nitrogen base, 2% glucose, and auxotrophic amino acids and vitamins as needed) as indicated. To induce autophagy, cells in the mid-log phase (OD_{600} = 0.8–1.0) were shifted to nitrogen-starvation medium with glucose (SD-N; 0.17% yeast nitrogen base without ammonium sulfate or amino acids, and 2% glucose) for the indicated times.

Plasmids

To generate the plasmids for the BiFC assay, the *CUP1* promoter was amplified from the pCu(416) plasmid (Labbe and Thiele, 1999)

and cloned into pRS405 and pRS406 vector plasmids. The VN fragment was polymerase chain reaction (PCR)-amplified from the pFA6a-VN-TRP1 plasmid (Sung and Huh, 2007) and inserted with the PCR-amplified open reading frame (ORF) of Big1 or Vma21 from the yeast genome after the *CUP1* promoter on the pRS405 vector. The VC fragment was PCR-amplified from pFA6a-VC-TRP1 (Sung and Huh, 2007) and inserted with the PCR-amplified ORF of *VPH1*, *VMA21*, or *VOA1* from the yeast genome or alone after the *CUP1* promoter on the pRS406 vector. The pRS405-CUP1p-GFP-ATG8 plasmid was constructed by replacing the endogenous *ATG8* promoter with the *CUP1* promoter and contains the open reading frame of GFP-Atg8 (Geng *et al.*, 2010). The pRS406-*BIG1p*-Big1-PA and pRS414-*BIG1p*-Big1-PA plasmids were constructed by inserting the endogenous *BIG1* promoter along with the ORF of *BIG1* into the pRS406 and pRS414 plasmid, respectively. The plasmid *pRS406-CUP1p-Big1-PA* was constructed by inserting the *CUP1* promoter along with the ORF of *BIG1* into the pRS406 plasmid. Similarly, the pRS406-*ZEO1p*-ATP6AP1 plasmid was constructed by inserting the *ZEO1* promoter along with the ORF of *ATP6AP1* into the pRS406 plasmid. Before transformation, pRS405-based plasmids were cut with AflII at 37°C, and pRS406-based plasmids were cut with BstBI at 65°C or StuI at 37°C.

AID* system

To set up the AID* system, WLY176 (WT) cells were first transformed with the plasmid pNHK53 (*ADH1p-OsTIR1-9MYC*). Big1 was then tagged with AID-9MYC by homologous recombination. The DNA fragments used for transformation were amplified with pHIS3-AID*-9MYC (Addgene, 99524; deposited by Dr. Helle Ulrich) as the template DNA. "AID*" refers to the 71–116 amino acids of the AT1G04250/IAA17 protein in plants (Morawska and Ulrich, 2013). To conditionally knock down *BIG1*, the cells were first cultured in YPD overnight until midlog phase and then diluted and treated with 300 μM IAA (Sigma, I2886) for the indicated time to induce the degradation of Big1. For starvation, cells were shifted to SD-N medium, and 300 μM IAA was added to the medium to maintain degradation of Big1. After an appropriate time period of treatment or starvation, samples were collected for western blot, qRT-PCR analysis or vacuole isolation.

Fluorescence microscopy

Cells were cultured in YPD until the midlog phase (OD_{600} = 0.8–1.0) and were then harvested and imaged. To label the vacuole as shown in Supplemental Figure S2B, SynaptoRedC2/FM 4-64 (Biotium) was added at a final concentration of 30 μM. Cells were stained at 30°C for 30 min, with shaking every 10 min. After staining, the cells were washed with YPD three times and then transferred into YPD for 1 h before imaging. Images were collected on a Leica DMi8 microscope with a 100 × objective and Leica Thunder imager. The projection of z-sections is shown in the figure.

Vacuole isolation and V-ATPase protein level detection

Vacuole isolation followed a previously published protocol (Haas, 1995). Briefly, after culturing in YPD overnight or after 12-h IAA or DMSO (control) treatment in YPD, ~1000 OD_{600} units of cells were collected and cells were resuspended in 50 ml wash buffer (0.1 M Tris-HCl, pH 9.4, 10 mM DTT). The cells were incubated at 30°C in a water bath for 10 min with occasional swirling. The cells were washed once with water and were then suspended in 30 ml spheroplasting buffer (50 mM potassium phosphate [a mixture of 0.8 M K_2HPO_4 and 0.2 M KH_2PO_4, pH 7.5] and 1.8 M sorbitol in 0.2 × YPD) with gentle vortexing. An appropriate amount of zymolyase (United States Biological, Z1005) was added and the tube was swirled to mix and incubated at 30°C until the OD_{600} reached 10–15% of that before the initiation of the zymolyase treatment. The tube was then centrifuged for 2 min at 1000 × *g* then the supernatant was removed. Spheroplasts were resuspended in 2.5 ml 15% ficoll (GE Healthcare, 17-0300-10) dissolved in PS buffer (20 mM PIPES, pH 6.8, 200 mM sorbitol). Dextran (200 μl, 2.5 mg/ml; MP Biomedicals, 195133) was added and the tube was put on ice for 3 min then in a 30°C water bath for 5 min. The vacuoles were floated on a four-tiered gradient of ficoll. The gradient was formed by pipetting 2.5–3 ml of the lysate in a 15% ficoll solution in the bottom of a high-speed centrifuge tube (Beckman, 344059). This initial layer was then overlayed with 3 ml 8% ficoll followed by 3 ml 4% ficoll and finally the tube was filled with 0% ficoll (PS buffer). The tubes were centrifuged at 32,000 rpm (Beckman Coulter OPTIMA L-90K ultracentrifuge, SW41 rotor) for 90 min at 4°C. The vacuoles were recovered from the interface between the 0% and 4% layers. The total protein amount of the isolated vacuoles was measured using the Pierce Bradford Protein Assay Kit (Thermo Fisher Scientific, 23200).

After culturing in YPD overnight or after 12-h IAA or DMSO (control) treatment in YPD, three OD_{600} units of cells were collected for total cell lysis preparation. Beads and lysis buffer (20 mM PIPES, pH 6.8, 50 mM KCl, 100 mM KOAc, 10 mM $MgSO_4$, 10 μM $ZnSO_4$, 0.5% Triton X-100 [Sigma, T8787]) were added and then the cells were vortexed for 5 min. The protein level in the supernatant was measured using the Pierce Bradford Protein Assay Kit. All of the protein samples (total cell lysis and vacuoles) were diluted in 4% ficoll to the same concentration in a final volume of 100 μl; 20 μl 2 × MURB (100 mM sodium phosphate, pH 7.0, 50 mM MES, pH 7.0, 2% SDS [w:v], 6 M urea, 2 mM NaN3, 2% β-mercaptoethanol, 0.02% bromophenol blue) was then added to each sample. The samples were boiled at 55°C for 15 min. The same amount of samples were loaded and resolved by SDS–PAGE.

V-ATPase activity

Total ATPase activity was measured using the ATPase Assay Kit (Abcam, ab270551). Bafilomycin A_1 (100 nM; Sigma, B1793) was used to specifically inhibit the V-ATPase activity. The V-ATPase activity is considered as the difference before and after $BafA_1$ inhibition. The assay plate was read using a Tecan Microplate Reader Infinite F200 at the wavelength of 660 nm.

RNA preparation and qRT-PCR

After 12-h IAA or DMSO (control) treatment in YPD and after 1-h starvation, one OD_{600} unit of cells was collected. The total RNA for each sample was isolated using the NucleoSpin RNA kit (Macherey-Nagel, 740955). One microgram of total RNA was subjected to reverse transcription using the High-Capacity cDNA Reverse Transcription kit (Applied Biosystems, 4368814). To analyze the cDNA levels, real-time PCR was performed with the Radiant Green Lo-ROX qPCR Kit (Alkali Scientific, QS1005) and run on the QuantStudio5 qPCR Machine (Thermo Fisher Scientific). The gene-specific primers for *ATG1*, *ATG7*, *ATG8*, *ATG9*, and *ATG41* and the reference gene *TAF10* are listed in previous studies (Hu *et al.*, 2015; Yao *et al.*, 2015).

Colony dot blot

The cells were cultured in YPD until midlog phase (OD_{600} = 0.8–1.0) and yeast cells were collected and diluted to 1.0 OD_{600}/ml; 8-fold serial dilutions were made in water. A 1.5 μl aliquot of each

dilution was spotted on a YPD plate at pH 5 or pH 7.5 containing 35 mM $CaCl_2$.

Co-immunoprecipitation

Cells were grown in 60 ml SMD-Trp medium at 30°C overnight. Cells (60 OD_{600} units) were harvested and washed with ice-cold 1 × PBS (137 mM NaCl, 2.7 mM KCl, 10 mM Na_2HPO_4, 1.8 mM KH_2PO_4, pH 7.4). The cell pellet for each sample was resuspended in 150 µL immunoprecipitation (IP) buffer (1 × PBS, 200 mM sorbitol, 1 mM $MgCl_2$, 0.5% Triton X-100, 1 mM PMSF and one tablet of proteinase inhibitor [Roche] in 50 ml IP buffer) and separated into four tubes. Glass beads were added into each tube and the samples were mixed by vortexing at 4°C and then centrifuged at 16,110 × *g* for 10 min. A 60-µL aliquot was taken from each sample as the input, and 1.2 ml supernatant was incubated with IgG Sepharose beads (GE Healthcare Life Sciences) at 4°C for 2 h. After incubation, the beads were washed with IP buffer six times. Next, 50 µl 2 × MURB was added to the beads and the beads were heated at 55°C for 15 min. The supernatants were resolved by SDS–PAGE. For the input samples, 1 ml 10% TCA was added, and the tube was placed on ice for 30 min. The input samples were then centrifuged at 16,110 × *g* and the pellets were washed with acetone and air-dried. A total of 50 µL 1 × MURB and glass beads were added to the pellet, followed by vortexing for 5 min. The samples were then heated at 55°C for 15 min and resolved by SDS–PAGE.

Western blot, antibodies, and antisera

Western blot was performed as described previously (Klionsky *et al.*, 2021). In Supplemental Figure S7A, p-Snf1was first blotted and then the membrane was washed twice with stripping buffer (1.5% glycine, 0.1% SDS, 1% Tween-20, pH 2.2) for 10 min at room temperature. Next, the membrane was washed with 1 × PBS twice for 10 min each time, followed by two washes for 5 min each with TBST (20 mM Tris, 150 mM NaCl, 0.1% Tween-20). After blocking with 5% milk in TBST, anti-HA antibody was used to blot total Snf1.

Anti-Pgk1 antiserum is a generous gift from Dr. Jeremy Thorner (University of California, Berkeley). Other antibodies were as follows: YFP, which detects GFP (Clontech, 63281), MYC/c-Myc (Sigma, M4439), Vph1 (Abcam, ab113683), Vma2 (Abnova, MAB14189), Prc1/CPY (Invitrogen, A-6428), HA (Sigma-Aldrich, H3663), PA (ImmunoResearch, 323-005-024), Dpm1 (Invitrogen, A-6429), p-Snf1 (Cell Signaling Technology, 2531), goat anti-rabbit IgG secondary antibody (Thermo Fisher Scientific, ICN55676), and rabbit anti-mouse IgG secondary antibody (Jackson, 315-035-003). Anti-Vma8 (Huang *et al.*, 2000), anti-Vma4 (Huang *et al.*, 2000), and anti-Atg1 (Abeliovich *et al.*, 2003) antibody were described previously.

Mammalian cell methods

HT1080 cells were cultured in DMEM (Thermo Fisher Scientific, 11995073) supplemented with 10% heat-inactivated FBS (Millipore, TMS-013-B) and 1% penicillin and streptomycin (Thermo Fisher Scientific, 15070-063) at 37°C, 95% humidity, and 5% CO_2. These cells were transfected with *ATP6AP1*-specific siRNAs (Sigma, SASI-Hs01-0015-1228 and SASI-Hs01-0015-1229) or a universal negative control (Sigma, SIC001) using Lipofectamine RNAiMAX (Invitrogen, 13778075). Transfections involved 100 pmol of siRNA per well in 6-well plates. After 48 h, protein levels were assessed by western blot using antibodies against ATP6AP1 and ACTB. To induce starvation, we used Hanks' balanced salt solution (HBSS; Thermo Fisher Scientific, 24020117) in the absence or presence of bafilomycin A_1 (Selleck Chemicals, S1413) after transfection for 48 h. Samples were collected after 0, 2, and 4 h of starvation and the protein levels were evaluated by western blot. Antibodies used were as follows: ATP6AP1 (Thermo Fisher Scientific, PA5-37328; 1:1000), ACTB (Cell Signaling Technology, 3700; 1:5000), SQSTM1 (Sigma, p0067; 1:1000), MAP1LC3/LC3 (Cell Signaling Technology, 4108; 1:1000).

Protein structure and interaction prediction

The predicted structure of Big1 was obtained from the AlphaFold database (https://alphafold.ebi.ac.uk/). The interaction between Big1 and Vph1 was predicted using ColabFold (Mirdita *et al.*, 2022). The model with the highest ranking is shown in the figure.

Statistical analysis

A two-tailed *t* test was used to determine statistical significance.

ACKNOWLEDGMENTS

This work was supported by NIH Grant GM131919 to DJK.

Author Disclosures

S.N.M. owns shares in Abbvie. The other authors declare no competing interests.

REFERENCES

Abeliovich H, Zhang C, Dunn WA Jr., Shokat KM, Klionsky DJ (2003). Chemical genetic analysis of Apg1 reveals a non-kinase role in the induction of autophagy. Mol Biol Cell 14, 477–490.

Azuma M, Levinson JN, Page N, Bussey H (2002). Saccharomyces cerevisiae Big1p, a putative endoplasmic reticulum membrane protein required for normal levels of cell wall beta-1,6-glucan. Yeast 19, 783–793.

Bartholomew CR, Suzuki T, Du Z, Backues SK, Jin M, Lynch-Day MA, Umekawa M, Kamath A, Zhao M, Xie Z, *et al.* (2012). Ume6 transcription factor is part of a signaling cascade that regulates autophagy. Proc Natl Acad Sci USA 109, 11206–11210.

Barua S, Berger S, Pereira EM, Jobanputra V (2022). Expanding the phenotype of ATP6AP1 deficiency. Cold Spring Harb Mol Case Stud 8, a006195.

Bernard A, Jin M, Xu Z, Klionsky DJ (2015). A large-scale analysis of autophagy-related gene expression identifies new regulators of autophagy. Autophagy 11, 2114–2122.

Chang YY, Neufeld TP (2009). An Atg1/Atg13 complex with multiple roles in TOR-mediated autophagy regulation. Mol Biol Cell 20, 2004–2014.

Chen F, Kang R, Liu J, Tang D (2022). The V-ATPases in cancer and cell death. Cancer Gene Ther 29, 1529–1541.

Colacurcio DJ, Nixon RA (2016). Disorders of lysosomal acidification-the emerging role of v-ATPase in aging and neurodegenerative disease. Ageing Res Rev 32, 75–88.

Compton MA, Graham LA, Stevens TH (2006). Vma9p (subunit e) is an integral membrane V0 subunit of the yeast V-ATPase. J Biol Chem 281, 15312–15319.

Crespo JL, Powers T, Fowler B, Hall MN (2002). The TOR-controlled transcription activators GLN3, RTG1, and RTG3 are regulated in response to intracellular levels of glutamine. Proc Natl Acad Sci USA 99, 6784–6789.

Gardner JM, Jaspersen SL (2014). Manipulating the yeast genome: deletion, mutation, and tagging by PCR. Methods Mol Biol 1205, 45–78.

Geng J, Nair U, Yasumura-Yorimitsu K, Klionsky DJ (2010). Post-Golgi Sec proteins are required for autophagy in Saccharomyces cerevisiae. Mol Biol Cell 21, 2257–2269.

Gueldener U, Heinisch J, Koehler GJ, Voss D, Hegemann JH (2002). A second set of loxP marker cassettes for Cre-mediated multiple gene knockouts in budding yeast. Nucleic Acids Res 30, e23.

Haas A (1995). A quantitative assay to measure homotypic vacuole fusion in vitro. Methods Cell Sci 17, 283–294.

Han X, Tang Y, Zhang Y, Zhang J, Hu Z, Xu W, Xu S, Niu Q (2022). Impaired V-ATPase leads to increased lysosomal pH, results in disrupted lysosomal degradation and autophagic flux blockage, contributes to fluoride-induced developmental neurotoxicity. Ecotoxicol Environ Saf 236, 113500.

Hill KJ, Stevens TH (1994). Vma21p is a yeast membrane protein retained in the endoplasmic reticulum by a di-lysine motif and is required for the

assembly of the vacuolar H(+)-ATPase complex. Mol Biol Cell 5, 1039–1050.
Hill KJ, Stevens TH (1995). Vma22p is a novel endoplasmic reticulum-associated protein required for assembly of the yeast vacuolar H(+)-ATPase complex. J Biol Chem 270, 22329–22336.
Hooper KM, Jacquin E, Li T, Goodwin JM, Brumell JH, Durgan J, Florey O (2022). V-ATPase is a universal regulator of LC3-associated phagocytosis and non-canonical autophagy. J Cell Biol 221, e202105112.
Hu G, McQuiston T, Bernard A, Park YD, Qiu J, Vural A, Zhang N, Waterman SR, Blewett NH, Myers TG, *et al.* (2015). A conserved mechanism of TOR-dependent RCK-mediated mRNA degradation regulates autophagy. Nat Cell Biol 17, 930–942.
Hu Z, Raucci S, Jaquenoud M, Hatakeyama R, Stumpe M, Rohr R, Reggiori F, De Virgilio C, Dengjel J (2019). Multilayered control of protein turnover by TORC1 and Atg1. Cell Rep 28, 3486–3496.e6.
Huang WP, Scott SV, Kim J, Klionsky DJ (2000). The itinerary of a vesicle component, Aut7p/Cvt5p, terminates in the yeast vacuole via the autophagy/Cvt pathways. J Biol Chem 275, 5845–5851.
Jackson DD, Stevens TH (1997). VMA12 encodes a yeast endoplasmic reticulum protein required for vacuolar H+-ATPase assembly. J Biol Chem 272, 25928–25934.
Jansen EJ, Timal S, Ryan M, Ashikov A, van Scherpenzeel M, Graham LA, Mandel H, Hoischen A, Iancu TC, Raymond K, *et al.* (2016). ATP6AP1 deficiency causes an immunodeficiency with hepatopathy, cognitive impairment and abnormal protein glycosylation. Nat Commun 7, 11600.
Kabeya Y, Kamada Y, Baba M, Takikawa H, Sasaki M, Ohsumi Y (2005). Atg17 functions in cooperation with Atg1 and Atg13 in yeast autophagy. Mol Biol Cell 16, 2544–2553.
Kamada Y, Yoshino K, Kondo C, Kawamata T, Oshiro N, Yonezawa K, Ohsumi Y (2010). Tor directly controls the Atg1 kinase complex to regulate autophagy. Mol Cell Biol 30, 1049–1058.
Kerppola TK (2006). Design and implementation of bimolecular fluorescence complementation (BiFC) assays for the visualization of protein interactions in living cells. Nat Protoc 1, 1278–1286.
Klionsky DJ, Abdel-Aziz AK, Abdelfatah S, Abdellatif M, Abdoli A, Abel S, Abeliovich H, Abildgaard MH, Abudu YP, Acevedo-Arozena A, *et al.* (2021). Guidelines for the use and interpretation of assays for monitoring autophagy (4th edition)[1]. Autophagy 17, 1–382.
Labbe S, Thiele DJ (1999). Copper ion inducible and repressible promoter systems in yeast. Methods Enzymol 306, 145–153.
Lee JH, Yu WH, Kumar A, Lee S, Mohan PS, Peterhoff CM, Wolfe DM, Martinez-Vicente M, Massey AC, Sovak G, *et al.* (2010). Lysosomal proteolysis and autophagy require presenilin 1 and are disrupted by Alzheimer-related PS1 mutations. Cell 141, 1146–1158.
Lei Y, Klionsky DJ (2022). The coordination of V-ATPase and ATG16L1 is part of a common mechanism of non-canonical autophagy. Autophagy 18, 2267–2269.
Liu X, Mao K, Yu AYH, Omairi-Nasser A, Austin J 2nd, Glick BS, Yip CK, Klionsky DJ (2016). The Atg17-Atg31-Atg29 complex coordinates with Atg11 to recruit the Vam7 SNARE and mediate autophagosome-vacuole fusion. Curr Biol 26, 150–160.
Louagie E, Taylor NA, Flamez D, Roebroek AJ, Bright NA, Meulemans S, Quintens R, Herrera PL, Schuit F, Van de Ven WJ, *et al.* (2008). Role of furin in granular acidification in the endocrine pancreas: identification of the V-ATPase subunit Ac45 as a candidate substrate. Proc Natl Acad Sci USA 105, 12319–12324.
Malkus P, Graham LA, Stevens TH, Schekman R (2004). Role of Vma21p in assembly and transport of the yeast vacuolar ATPase. Mol Biol Cell 15, 5075–5091.
Mirdita M, Schutze K, Moriwaki Y, Heo L, Ovchinnikov S, Steinegger M (2022). ColabFold: making protein folding accessible to all. Nat Methods 19, 679–682.
Morawska M, Ulrich HD (2013). An expanded tool kit for the auxin-inducible degron system in budding yeast. Yeast 30, 341–351.
Morgan JT, Fink GR, Bartel DP (2019). Excised linear introns regulate growth in yeast. Nature 565, 606–611.
Nishimura K, Fukagawa T, Takisawa H, Kakimoto T, Kanemaki M (2009). An auxin-based degron system for the rapid depletion of proteins in non-plant cells. Nat Methods 6, 917–922.
Okosun J, Wolfson RL, Wang J, Araf S, Wilkins L, Castellano BM, Escudero-Ibarz L, Al Seraihi AF, Richter J, Bernhart SH, *et al.* (2016). Recurrent mTORC1-activating RRAGC mutations in follicular lymphoma. Nat Genet 48, 183–188.
Pareja F, Brandes AH, Basili T, Selenica P, Geyer FC, Fan D, Da Cruz Paula A, Kumar R, Brown DN, Gularte-Merida R, *et al.* (2018). Loss-of-function mutations in ATP6AP1 and ATP6AP2 in granular cell tumors. Nat Commun 9, 3533.
Roh SH, Stam NJ, Hryc CF, Couoh-Cardel S, Pintilie G, Chiu W, Wilkens S (2018). The 3.5-A CryoEM structure of nanodisc-reconstituted yeast vacuolar ATPase V(o) proton channel. Mol Cell 69, 993–1004.e3.
Ryan M, Graham LA, Stevens TH (2008). Voa1p functions in V-ATPase assembly in the yeast endoplasmic reticulum. Mol Biol Cell 19, 5131–5142.
Saiz-Baggetto S, Mendez E, Quilis I, Igual JC, Bano MC (2017). Chimeric proteins tagged with specific 3xHA cassettes may present instability and functional problems. PLoS One 12, e0183067.
Sambade M, Alba M, Smardon AM, West RW, Kane PM (2005). A genomic screen for yeast vacuolar membrane ATPase mutants. Genetics 170, 1539–1551.
Schmidt A, Beck T, Koller A, Kunz J, Hall MN (1998). The TOR nutrient signalling pathway phosphorylates NPR1 and inhibits turnover of the tryptophan permease. EMBO J 17, 6924–6931.
Soding J, Biegert A, Lupas AN (2005). The HHpred interactive server for protein homology detection and structure prediction. Nucleic Acids Res 33, W244–W248.
Sung MK, Huh WK (2007). Bimolecular fluorescence complementation analysis system for in vivo detection of protein-protein interaction in Saccharomyces cerevisiae. Yeast 24, 767–775.
Urban J, Soulard A, Huber A, Lippman S, Mukhopadhyay D, Deloche O, Wanke V, Anrather D, Ammerer G, Riezman H, *et al.* (2007). Sch9 is a major target of TORC1 in Saccharomyces cerevisiae. Mol Cell 26, 663–674.
Wang F, Gatica D, Ying ZX, Peterson LF, Kim P, Bernard D, Saiya-Cork K, Wang S, Kaminski MS, Chang AE, *et al.* (2019). Follicular lymphoma-associated mutations in vacuolar ATPase ATP6V1B2 activate autophagic flux and mTOR. J Clin Invest 129, 1626–1640.
Wang F, Yang Y, Boudagh G, Eskelinen EL, Klionsky DJ, Malek SN (2022). Follicular lymphoma-associated mutations in the V-ATPase chaperone VMA21 activate autophagy creating a targetable dependency. Autophagy 18, 1982–2000.
Wang H, Bueler SA, Rubinstein JL (2023). Structural basis of V-ATPase V(O) region assembly by Vma12p, 21p, and 22p. Proc Natl Acad Sci USA 120, e2217181120.
Wang H, Rubinstein JL (2023). CryoEM of V-ATPases: assembly, disassembly, and inhibition. Curr Opin Struct Biol 80, 102592.
Wang L, Wu D, Robinson CV, Wu H, Fu TM (2020). Structures of a complete human V-ATPase reveal mechanisms of its assembly. Mol Cell 80, 501–511.e3.
Xu Y, Zhou P, Cheng S, Lu Q, Nowak K, Hopp AK, Li L, Shi X, Zhou Z, Gao W, *et al.* (2019). A bacterial effector reveals the V-ATPase-ATG16L1 axis that initiates xenophagy. Cell 178, 552–566.e20.
Yao Z, Delorme-Axford E, Backues SK, Klionsky DJ (2015). Atg41/Icy2 regulates autophagosome formation. Autophagy 11, 2288–2299.